Environmental Science and Pollution Research (2023) 30:38713–38727
https://doi.org/10.1007/s11356-022-25033-x

RESEARCH ARTICLE

# Mechanical mechanism of rib spalling and sensitivity analysis of gangue parameters to rib spalling in gangue-bearing coal seams

**Guosheng Li[1] · Zhenhua Li[1,2] · Feng Du[1,2] · Zhengzheng Cao[3]**

Received: 13 June 2022 / Accepted: 24 December 2022 / Published online: 31 December 2022


## Abstract

Rib spalling is one of the main factors restricting the safe and efficient production of the fully mechanized mining face in gangue-bearing coal seams, and the gangue has significant influence on the occurrence of rib spalling. In this study, the instability process and mechanical mechanism of rib spalling in gangue-bearing coal seams were studied, and the sensitivity of gangue parameters to rib spalling was analyzed. The simulation test of rib spalling under different gangue parameters was carried out by orthogonal tests. The width and depth of rib spalling were taken as evaluation indexes, and the influence of gangue parameters on the rib spalling was analyzed by variance analysis and significance tests. The results show that the failure process of rib spalling is characterized by the fracturing failure of the lower coal body, shear failure of the gangue layer, and the falling off of the upper coal body caused by the gravity; the gangue parameters (thickness, density, joint inclination, and internal friction angle) have an important influence on the sliding instability of the coal wall. In the sensitivity analysis, the influence of gangue parameters on the width of rib spalling is ordered as gangue density > joint inclination > gangue thickness > internal friction angle; the influence of gangue parameters on the depth of rib spalling is ordered as gangue density > joint inclination > internal friction angle > gangue thickness. Besides, the greater the gangue density, the less damage caused by stress concentration, and the lower the risk of rib spalling.

**Keywords** Gangue-bearing coal seams · Slip instability · Gangue parameters · Sensitivity analysis · Orthogonal tests · Variance analysis

## Introduction

Thick coal seams are mainly extracted in the large coal bases of China, and thick coal seam mining is the main technical means to realize high-yield and efficient mining in China (Yu et al. 2015 and Song et al. 2015). With the gradual improvement of coal mining equipment and production management, the mining thickness of the working face also gradually increases, resulting in the change of stope stress and the difficulty in the stability control of coal walls. In this case, the accidents such as rib spalling and roof flaking are easily caused, which threatens the safety of personnel and equipment in the working face and seriously affects the production of coal mines (Tewari et al. 2018, Majdi et al. 2012 and Shabanimashcool and Li 2012).

In recent years, researchers have conducted in-depth research on the causes, formation process, and prevention technology of rib spalling in coal mining face, and studied the characteristics, mechanism, and control measures of rib spalling. The formation mechanism and influencing factors of rib spalling are analyzed,

Responsible Editor: Shimin Liu

**Highlights**
- This study ananlyzed the structural instability and failure process of gangue-bearing coal seams
- This study ananlyzed the mechanical mechanism of gangue parameters on the rib spalling of gangue-bearing coal seams
- Variance analysis and significance test are used to analyze the sensitivity of gangue parameters to the width and depth of rib spalling

✉ Zhenhua Li
jzlizhenh@163.com

[1] School of Energy Science and Engineering, Henan Polytechnic University, Jiaozuo 454000, Henan, China

[2] Collaborative Innovation Center of Coal Work Safety and Clean High Efficiency Utilization, Jiaozuo 454000, Henan, China

[3] School of Civil Engineering, Henan Polytechnic University, Jiaozuo 454003, Henan, China

and relieving the roof pressure of coal walls is the most effective measure to prevent the failure of coal walls (Wang et al. 2015 and Liu et al. 2020, 2021). There is a great relationship between rib spalling and coal wall support strength, and obtained the relationship expression between them (Ma et al. 2022a, b, c and Guo et al. 2019). Stability of coal face are mainly affected by coal cutting height, support strength, coal friction, and so on (Kong et al. 2019a, b). A safety evaluation system is developed for the mechanical models of coal wall instability under different wall trace lines (Yin et al. 2015). The influence of the working face dip angle on rib spalling, and found that the deformation of rock beam in the middle and upper part of the working face was the largest, this study reveals the influence mechanism of mining thickness on coal wall stability (Behera et al. 2020 and Zhu et al. 2021). The spalling characteristics of coal wall rib in large dip angle and mining height is mainly shear slip failure mode (Lu et al. 2019 and Wu et al. 2016). Mining failure surface of hard coal in the jointed coal seam is the conjugate surface composed of shear failure surface and joint tensile failure surface (Yang et al. 2012 and Li et al. 2022). The quantitative expression of limit equilibrium boundary of top coal is obtained through mechanical analysis of continuous failure medium (Lang et al. 2021). Grouting reinforcement becomes one of the main technical means to prevent and control coal wall spalling, which identifies a grouting material for coal seam floor crack reinforcement with good usage effect (Zhang et al. 2019). The mechanical model of coal wall slip instability was established and the risk coefficient equation of slip on the slip surface was deduced (Liu et al. 2019, Wang et al. 2021 and Li et al. 2020). Through theoretical analysis and numerical simulation, the spatial location of coal wall prone to sliding failure is analyzed (Bai et al. 2014, 2016 and Yao et al. 2017).

At present, the research on rib spalling in thick gangue-bearing coal seams mainly focuses on the characteristics, influencing factors, and prevention measures of rib spalling. However, there is the lack of in-depth research on the mechanism of the gangue itself on the coal wall of the gangue-bearing coal seam. Therefore, this paper discusses the destabilization mechanical process and sensitivity degree of gangue parameters on the coal wall flake gang of gangue-bearing coal seam, the width and depth of the rib spalling were taken as evaluation indexes, and the sensitivity of the gangue parameters to the rib spalling of gangue-bearing coal seams was analyzed by numerical calculation and theoretical analysis. This study provides a meaningful theoretical basis for the prevention and control measures of the rib spalling of the thick coal seam.

## Rib spalling characteristics and main gangue parameters in the working face

Under different mining parameters and stress conditions, the coal wall presents different forms of rib spalling. According to the different occurrence positions, rib spalling can be divided into upper rib spalling, middle rib spalling, and middle-upper rib spalling (Xu et al. 2021a, b). Buertai coal mine is located in Ordos City, Inner Mongolia Autonomous Region, China, and it is known through the on-site observation of 42,105 working face in mining area 1 of Buertai coal mine. Figure 1 shows the coal wall failure observed in the on-site working face of gangue-bearing coal seams in the Buertai coal mine. The working face is supported by hydraulic supports, and 115 hydraulic supports are arranged in the whole working face, including 103 middle supports and 12 auxiliary supports. The middle support selects ZFY18000/25/39D double-column shield top-coal caving hydraulic support produced by Zhengzhou coal machine. From the field observation, it can be found that the slabbing rid spalling mainly occurs in the middle of the coal wall. Referring to the research on the slabbing rib spalling of the coal wall in the existing working face (Zhou et al. 2015, Diederichs et al. 2004 and Du et al. 2015), it is concluded that the occurrence of the slabbing rib spalling is closely related to the hardness of coal seams, mining height of the working face, mine pressure, support strength, equipment management, and other factors. The essence of rib spalling is the process that the coal wall breaks its original stability and collapses into the working face under the comprehensive action of multiple factors. If some special circumstances are encountered, such as complex geological conditions, basic roof weighting, improper selection of mining techniques, and insufficient equipment management, then rib spalling is easily caused after the tensile stress or shear stress of the coal wall exceeds its limit bearing capacity. It can be seen from the field diagram that due to the different thickness of the gangue in different positions of the coal seam, the stability of the coal wall also shows a large difference, indicating that the change of the gangue parameters has an important influence on the stability of the coal wall of the working face.

Figure 2 shows the schematic diagram of rib spalling in the working face. According to the above analysis, the main control factors affecting the occurrence of rib spalling in the gangue-bearing coal seams are as follows. (1) Gangue density. The greater the density of the gangue layer, which means that the unit volume of the gangue gravity increases, to ensure that the geological conditions are the same case, the greater the density of the parting coal wall spalling possibility. (2) Gangue thickness. The greater the thickness of the gangue layer, the higher the proportion of gangue in the whole coal wall height, the lower the proportion of the weak surface (coal seam) and the possibility of rib spalling. (3) Internal friction angle, the change of internal friction angle changes the strength of the gangue layer, which affects the range of the potential rib spalling. (4) Joint inclination. The greater the joint inclination of the gangue layer, the greater the downward tensile stress component, and the greater the possibility of gangue slip.

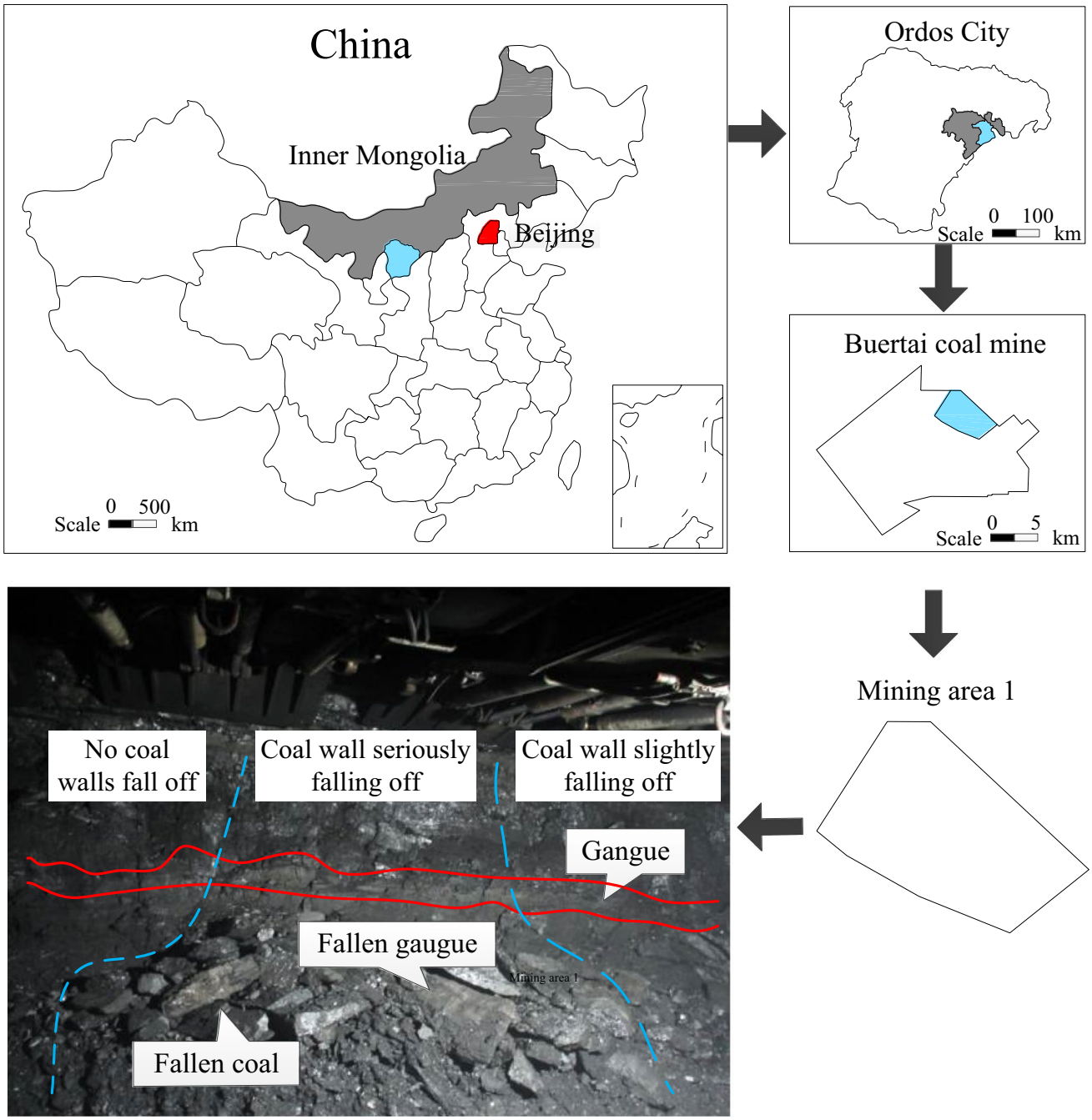


**Fig. 1** Geographical location of the working face and the site map of the coal wall rib spalling

## Methods

### Mechanical mechanism and sliding instability of coal wall failure in gangue-bearing coal seams

#### Analysis of structural instability and failure process of gangue-bearing coal seams

According to the macroscopic instability model of gangue-bearing coal seams in the working face, with the advancement of the working face, the advanced stress of the working face significantly increases the static load stress of gangue-bearing coal seams, and the breaking of the roof structure releases the dynamic load stress, as shown in Fig. 2. In addition, the gas stress inside the coal seam will also provide energy for the coal to move outward. At the same time, the mining of the working face provides a space for coal deformation. Therefore, under the superposition of

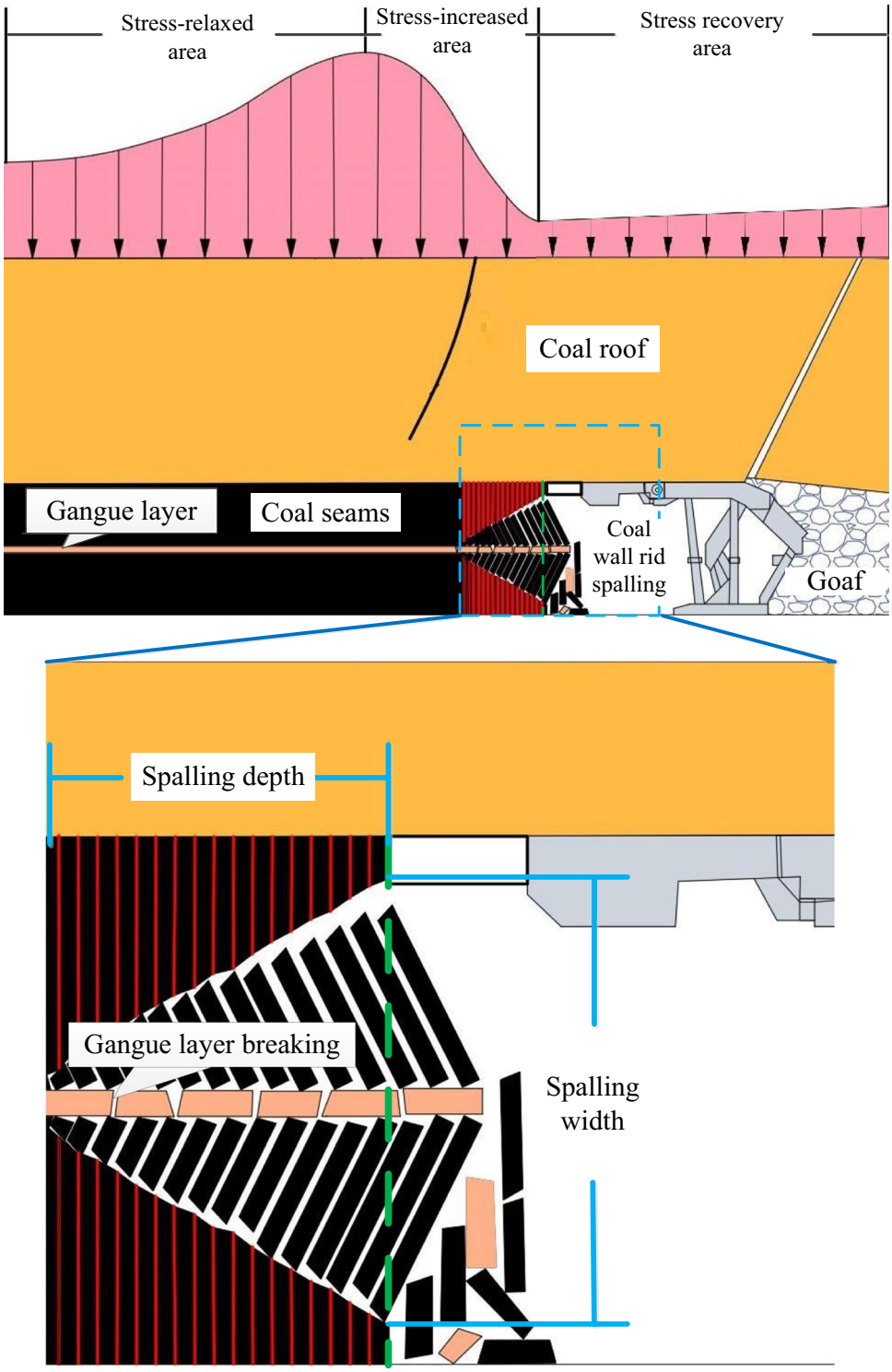


**Fig. 2** Site map of rib spalling in the working face

static load stress, dynamic load stress, and gas stress, the instability failure of gangue-bearing coal seams is caused.

For simplicity, the coal body below the gangue is called the lower coal body, and the coal body above the gangue is the upper coal body. As shown in Fig. 3, due to the difference in the spatial relationship of the coal body, the static load stress of the lower coal body is larger than that of the upper coal body. Under the simultaneous action of large static load stress advanced stress and gas stress, a large number of cracks in the lower coal body are better developed, and the crack connection is easily caused, resulting in the fracturing failure of the lower coal body. Subsequently,

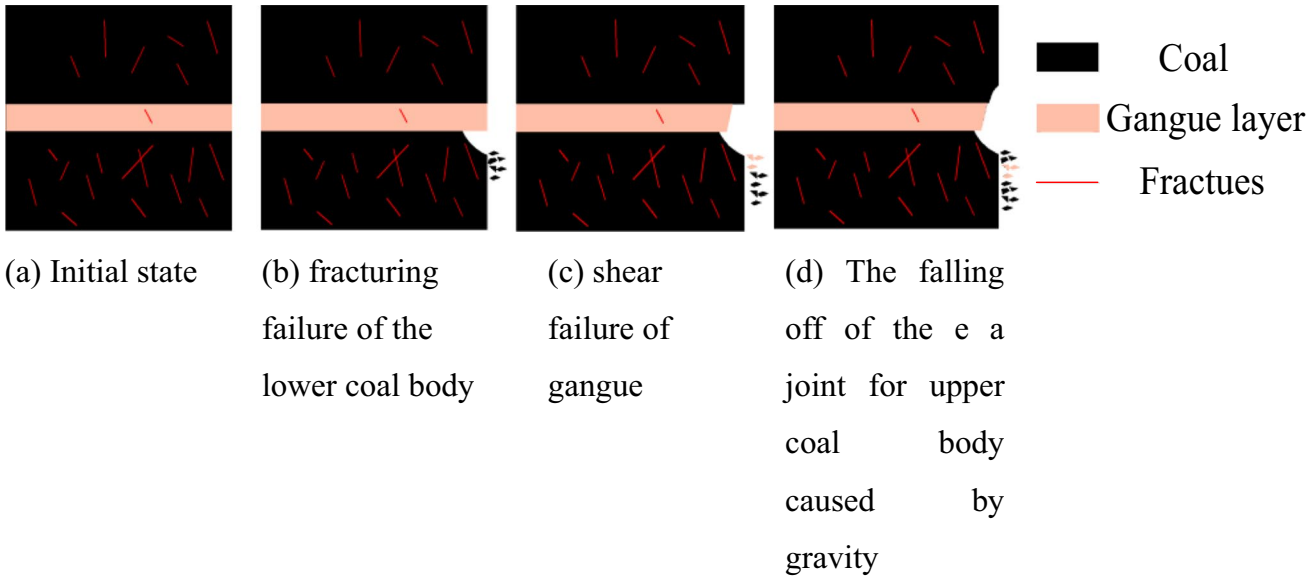


**Fig. 3** Schematic diagram of structural failure process of gangue-bearing coal seams

the shear failure of the gangue layer can be induced due to the static load stress. Finally, after losing the support of the gangue layer, the upper coal body falls off by gravity. In summary, the failure order of the coal wall is as follows: fracturing failure of the lower coal body, shear failure of the gangue layer, and fall off of the upper coal body caused by gravity.

### Mechanical mechanism of sliding instability of structural plane of gangue layer

Based on the occurrence characteristics of the gangue-wearing coal seams in this analysis, it is assumed that the gangue is located in the middle of the coal seam, the thickness remains unchanged, and the inclination angle of the contact surface between the coal body and the gangue is 0; thus, there is no risk of sliding and instability (see Fig. 3). If there is a joint forming an angle $\beta$ ($0 \le \beta < \pi/2$) with the outer normal of the horizontal main plane in the gangue layer (see Fig. 4), under the action of roof pressure, the gangue with perforating structural plane may be destroyed along the structural plane path. Here, it is assumed that: (1) the gangue layer is an isotropic homogeneous body; (2) the sliding instability of its structural plane meets the Mohr–Coulomb strength criterion; (3) the horizontal and vertical directions are the main planes, $\sigma_1$ and $\sigma_3$ are main stress, and the maximum and minimum principal stresses are not distinguished; (4) $\sigma$ and $\tau$ are the normal stress and shear stress on the structural plane, and the bonding force $c$ between the structural planes is 0.

The plane mechanical model is established by taking rectangular micro elements at the structural plane of

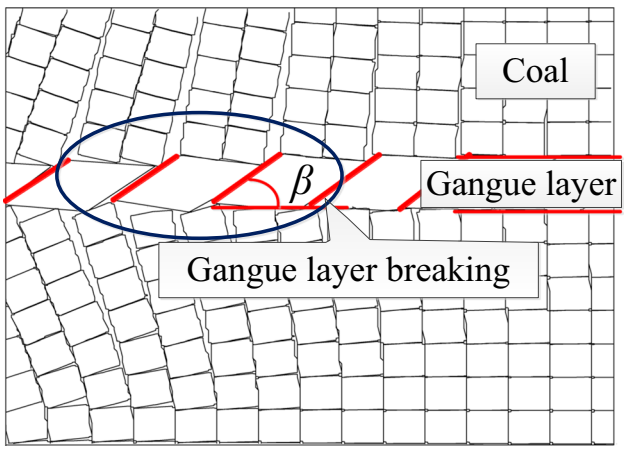


**Fig. 4** Schematic diagram of failure of the structural plane in the gangue layer

gangue-bearing coal rock, as shown in Fig. 5a. Based on the Mohr–Coulomb friction law (Shen and Chen 2006), the sliding shear strength limit of a structural plane is:

$$\left| \frac{(\sigma - \tau)\sin 2\beta}{(\sigma_1 + \sigma_3) + (\sigma_1 - \sigma_3)\cos 2\beta} = \tan\varphi_c \right| \tag{1}$$

where $\varphi_c$ is the internal friction angle of the structural plane.

According to the Mohr–Coulomb criterion, the mechanical relationship between the load applied above the gangue layer and the strength curve of the structural plane can be represented by the Mohr stress circle, as shown in Fig. 5b. It can be seen that when the failure occurs along the structural plane, the strength curve of the structural plane intersects

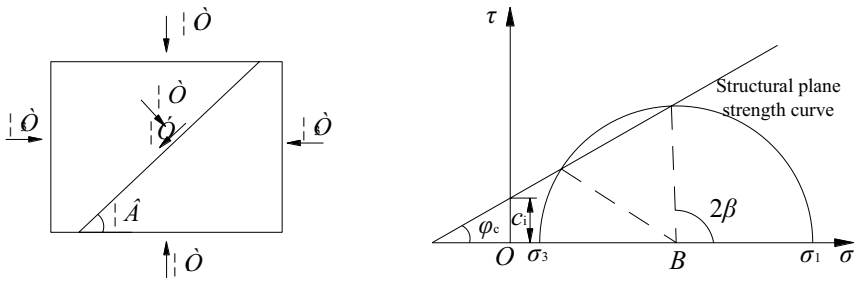


**Fig. 5** Mechanical analysis of the structural plane

(a) Plane mechanics diagram of rectangular micro element (b) Mohr stress circle

with the point representing the stress state of the structural plane.

According to the geometric relationship between the strength curve of structural plane and the Mohr stress circle, the strength equation of structural plane is deduced as follows:

$$\frac{\sigma_1-\sigma_3}{2}\sin\ 2\beta = c_i + \left(\frac{\sigma_1+\sigma_3}{2} + \frac{\sigma_1-\sigma_3}{2}\cos 2\beta\right)\tan\varphi_c \tag{2}$$

Through proper simplification, Eq. (3) can be obtained.

$$\sigma_1-\sigma_3 = \frac{2\sigma_3\tan\varphi_c + 2c_i}{\left(1-\tan\varphi_c\cot\beta\right)\sin\ 2\beta} \tag{3}$$

It can be concluded that the angle $\beta$ between the structural plane and the maximum principal stress plane acts on the maximum principal stress, only the angle $\beta$ satisfies: (1) $\beta \to \varphi_i$ or $\beta \to \pi/2, \sigma_1 \to \infty$; (2) only when $\varphi_i < \beta < \pi/2$, the structural plane failure may occur.

When the normal stress acting on the structural plane gradually increases, the strength of the structural plane also increases. Therefore, the intersection points of the strength line and the stress circle can be obtained, which corresponds to the angles $\beta_1$ and $\beta_2$ of the structural plane.

$$2\beta_1 = \pi + \varphi_c - \arcsin\left\{\left[\left(\frac{\sigma_\mathrm{m}+c_i\cot\varphi_c}{\tau_\mathrm{m}}\right)\right]\sin\varphi_c\right\} \tag{4}$$

$$2\beta_2 = \varphi_c + \arcsin\left\{\left[\left(\frac{\varphi_\mathrm{m}+c_i\cot\varphi_c}{\tau_\mathrm{m}}\right)\right]\sin\varphi_c\right\} \tag{5}$$

According to the physical significance of $\beta_1$ and $\beta_2$, when the angle $\beta$ of the structural plane ranges between $\beta_1$ and $\beta_2$, the structural plane of the gangue layer is damaged. When the angle $\beta$ of gangue layer is within $\beta_1$ and $\beta_2$, the mechanical mechanism of structural plane sliding instability is analyzed.

According to the spatial distribution characteristics of the advanced stress of the working face, the peak stress is generally a certain distance ahead of the working face, and the probability of structural instability of the gangue layer in the coal body is high, resulting in the empty state of the gangue on the side of the coal. Based on the stress of the upper and lower coal seams, the mechanical analysis of the gangue layer is carried out. As shown in Fig. 6, the vertical height between the structural plane and the solid coal above ($H$) is composed of two parts: the thickness of gangue layer ($H_1$) and the vertical height between the upper boundary of gangue and solid coal ($H_2$); $F(h)$ and $K(h)$ are the horizontal normal stress and vertical shear stress acting on the structural plane by the combination of coal and gangue, and $AB$ is the structural plane of gangue layer. In the stable state, the combination of coal and gangue is in the equilibrium state, and the mechanical equilibrium equation is established as follows:

$$\sum F_x = 0, \sum F_y = 0, \sum M_o = 0 \tag{6}$$

Then, it can be obtained that:

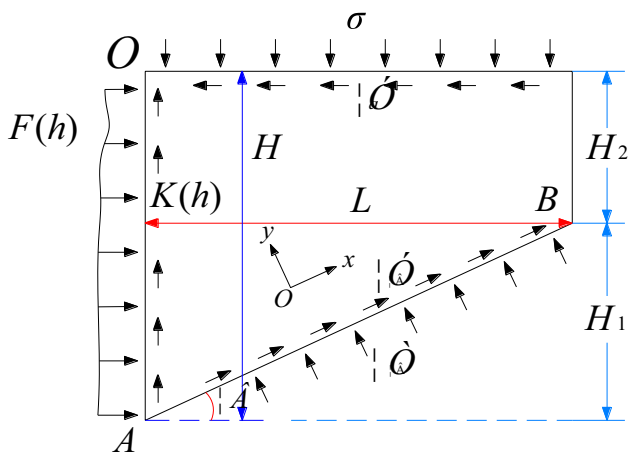


**Fig. 6** Stress on gangue structural plane (*AB* is the structural plane)

$$\left.\begin{array}{l}\frac{\tau_\beta L}{\cos\beta}+\int_0^{H_1+H_2}F(h)\cos\beta\,dh+\int_0^{H_1+H_2}K(h)\sin\beta\,dh-\tau_a L\cos\beta-\sigma L\sin\beta=0\\ \frac{\sigma_\beta L}{\cos\beta}-\int_0^{H_1+H_2}F(h)\sin\beta\,dh+\int_0^{H_1+H_2}K(h)\cos\beta\,dh+\tau_a L\cos\beta-\sigma L\cos\beta=0\\ \frac{\sigma_\beta L}{\cos\beta}\left(\frac{L}{2\cos\beta}-H_1\sin\beta\right)+\frac{\tau_\beta L}{\cos\beta}(H_1+H_2)\cos\beta+\int_0^{H_1+H_2}F(h)h\,dh-\frac{\sigma L^2}{2}=0\end{array}\right\}\quad(7)$$

Supposing that the horizontal normal stress and vertical shear stress of the gangue structure plane subjected to the combination are uniformly distributed loads, which are defined as $d_1\sigma$ and $d_2\tau_a$, respectively. Then the equation can be simplified as follows:

$$\left.\begin{array}{l}\frac{\tau_\beta L}{\cos\beta}+d_1\sigma H\cos\beta+d_2\tau_a(H)\sin\beta-\tau_a L\cos\beta\\ -\sigma L\sin\beta=0\\ \frac{\sigma_\beta L}{\cos\beta}-d_1\sigma H\sin\beta+d_2\tau_a H\cos\beta+\tau_a L\cos\beta\\ -\sigma L\cos\beta=0\\ \frac{\sigma_\beta L}{\cos\beta}\left(\frac{L}{2\cos\beta}-H_1\sin\beta\right)+\frac{\tau_\beta L}{\cos\beta}H\cos\beta\\ +\frac{d_1\sigma H^2}{2}-\frac{\sigma L^2}{2}=0\end{array}\right\}\quad(8)$$

Equation (9) can be obtained.

$$\left.\begin{array}{l}\tau_\beta=\sigma\sin\beta\cos\beta-\frac{d_1 H\sigma}{L}\cos^2\beta+\tau_a\cos^2\beta\\ -\frac{d_2 H\tau_a}{L}\sin\beta\cos\beta\\ \tau_\beta=\sigma\cos^2\beta+\frac{d_1 H\sigma}{L}\sin\beta\cos\beta-\tau_a\sin\beta\cos\beta\\ -\frac{d_2 H\tau_a}{L}\cos^2\beta\\ \tau_a=\frac{d_1(H-L\tan\beta)\sigma}{L[2H-\lambda H-L\tan\beta]}\end{array}\right\}\quad(9)$$

According to Eq. (9), the ratio of shear stress to normal stress on the structural plane can be obtained as follows:

$$\left.\begin{array}{l}\frac{\tau_\beta}{\sigma_\beta}=\frac{\sigma\sin\beta\cos\beta-\frac{d_1 H\sigma}{L}\cos^2\beta+D_1}{\sigma\cos^2\beta+\frac{d_1 H\sigma}{L}\sin\beta\cos\beta-D_2}\\ D_1=\tau_a\cos^2\beta-\frac{d_2 H\tau_a}{L}\sin\beta\cos\beta\\ \frac{\tau_\beta}{\sigma_\beta}=\frac{\sin\beta(L\sigma-d_2 H)+\cos\beta(L\tau_a-d_1 H)}{\sin\beta(d_1 H\sigma-\tau_a L)+\cos\beta(L\sigma-d_2 H\tau_a)}\end{array}\right\}\quad(10)$$

In the Eq. (10), H can be expressed as follows:

$$H=H_1+H_2, L=H_1/\tan\beta\quad(11)$$

where $\sigma$ is the vertical stress of gangue $\sigma_1$ and its own gravity $G_j$. The value of $G_j$ is related to gangue density $\rho_j$ and gangue volume $V_j$, and $G_j$ can be expressed as follows:

$$G_j=\rho_j V_j\quad(12)$$

Then, it can be obtained that:

$$\sigma=\sigma_1+G_j=\sigma_1+\rho_j V_j\quad(13)$$

From Eqs. (9)–(13), the discrimination formula of sliding instability of gangue and coal combined structure on gangue structural plane can be introduced as follows:

$$f(H_1,H_2,\beta,\rho_j)=\frac{\sin\beta[H_1(\sigma_1+\rho_j V_j)/\tan\beta-d_2(H_1+H_2)]+\cos\beta[H_1\tau_a/\tan\beta-d_1(H_1+H_2)(\sigma_1+\rho_j V_j)]}{\sin\beta[d_1(H_1+H_2)(\sigma_1+\rho_j V_j)-\tau_a H_1/\tan\beta]+\cos\beta[H_1(\sigma_1+\rho_j V_j)/\tan\beta-d_2(H_1+H_2)\tau_a]}\quad(14)$$

According to Mohr–Coulomb friction law, the judgment condition of relative sliding instability of gangue layer on the structural plane is:

$$f(H_1,H_2,L,\rho_j)=\frac{\sin\beta[L(\sigma_1+\rho_j V_j)-d_2(H_1+H_2)]+\cos\beta[L\tau_a-d_1(H_1+H_2)(\sigma_1+\rho_j V_j)]}{\sin\beta[d_1(H_1+H_2)(\sigma_1+\rho_j V_j)-\tau_a L]+\cos\beta[L(\sigma_1+\rho_j V_j)-d_2(H_1+H_2)\tau_a]}\geq\tan\varphi_c\quad(15)$$

It should be noted that when discussing the influence of each gangue parameter on the sliding instability of the gangue layer, it is necessary to ensure that other parameters remain unchanged. According to the formula (15), with the increase of the dip angle of the structural plane $\beta$, the $f$ value will gradually increase, which means that the possibility of relative slip instability of the gangue layer is higher. On the contrary, with the increase of internal friction angle $\varphi_c$, the possibility of relative slip instability is lower. With the increase of thickness $H_1$, the value of $f$ will decrease gradually, and the possibility of relative slip instability of the gangue layer is smaller. With the increase of density $\rho_j$, the value of $f$ will become larger, and the possibility of relative slip instability will increase. As shown in Eq. (15), the relative sliding instability of the gangue layer on the structural plane is mainly affected by the inclination of the structural plane $\beta$, internal friction angle $\varphi_c$, thickness $H_1$ and density $\rho_j$, and other parameters. The changes in these parameters affect the occurrence of the sliding instability of the gangue structural plane and its sliding degree, resulting in differences in the depth and width of rib spalling. Therefore, it is necessary to study the sensitivity of structural plane parameters (such as joint inclination and internal friction angle of gangue layer) and physical parameters (such as thickness and density of gangue) to the occurrence of rib spalling.

## Establishment of numerical model of rib spalling and scheme determination

### Establishment of numerical model

According to the field mining situation and numerical calculation of the Buertai coal mine, the numerical model is simplified, and the simplified simulation diagram is shown in Fig. 7. Considering the influence range of main factors, the UDEC discrete element calculation software is used for the numerical simulation. The average buried depth of coal seam is set as 450 m, the thickness of the coal seam is 6.7 m, the mining height is 3.7 m, and the top coal caving is 3 m. Besides, the size required for numerical simulation was determined as length ($x$) × height ($y$) = 140 m × 52.5 m. The left, right, and bottom boundaries of the numerical model

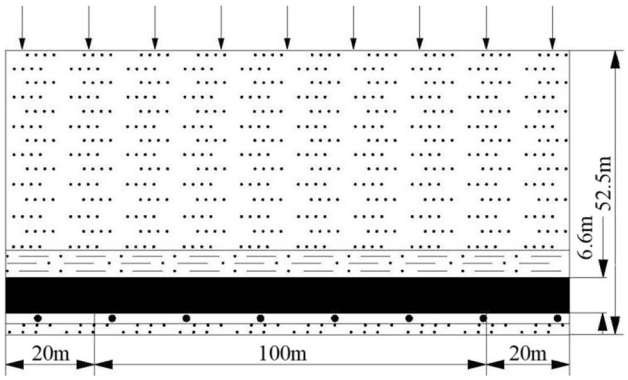


**Fig. 7** Schematic diagram of working face mining

are displacement boundaries. Specifically, left and right boundaries limit horizontal displacement, and the bottom boundary limits vertical displacement. The upper boundary is the free boundary, and an equivalent load is applied to the upper boundary of the model. The equivalent load of overburden rock is calculated by formula $F=\lambda H=\rho_p gH$, where $\lambda$ is the average unit weight of overburden rock, N/m$^3$. $\rho_p$ is the average density of overlying strata, which is 2060 kg/m$^3$. $g$ is the acceleration of gravity, which is 9.8 m/s$^2$. $H$ is the average buried depth of coal seam, which is 450 m from the front, therefore, $F=9$ MPa is calculated. In this simulation, it is assumed that the gangue layer is located in the middle of the coal seam, and the calculation model is shown in Fig. 8.

The staged excavation is performed in the coal seam, with each excavation of 10 m and a total of 100 m. The 20-m coal pillars are reserved on both sides of the model. On the premise of meeting the accuracy and effectiveness of the calculation, the composition of rock strata within the scope of the calculation model is simplified, and the rock strata with similar physical properties are treated as single rock formations. According to the field mining data, the model is divided into 5 layers, and the lithology parameters of each rock stratum are shown in Table 1.

## Simulation scheme

The purpose of this study is to determine the sensitivity of gangue parameters to the influence range (depth and width) of rib spalling. Due to a large number of numerical simulation calculation models and influencing factors, single calculation will result in complicated calculation. To effectively reduce the workload of calculation, the orthogonal experimental method (Chen 2005) was adopted to determine the experimental simulation scheme by designing the orthogonal table. Through the above analysis of the influence of the

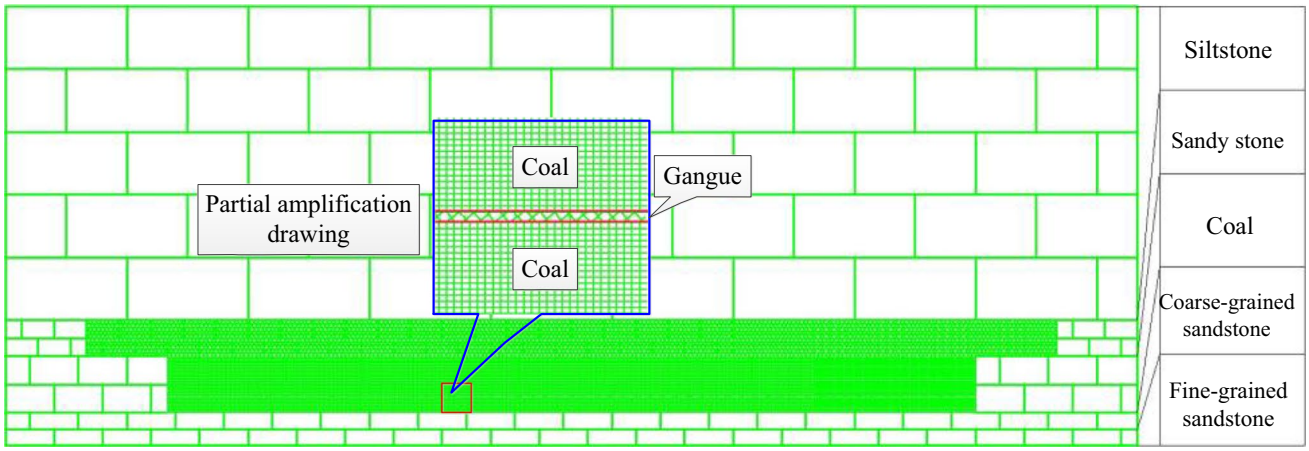


**Fig. 8** The numerical calculation model

**Table 1** Physical and mechanical parameters of coal rock

| Lithology | Thickness (m) | Density (g/cm$^3$) | Tensile strength (MPa) | Cohesion (MPa) | Internal friction angle (°) |
|---|---|---|---|---|---|
| Siltstone | 37.1 | 2325 | 4.89 | 22.43 | 27 |
| Sandy mudstone | 4.31 | 2403 | 6.66 | 27.79 | 26 |
| Coal | 6.56 | 1274 | 1.38 | 2.51 | 30 |
| Coarse-grained sandstone | 1.98 | 2232 | 2.04 | 8.65 | 28 |
| Fine-grained sandstone | 1.99 | 2301 | 5.61 | 30.91 | 20 |

gangue parameters on the rib spalling, the main control factors of the gangue are the gangue thickness, gangue density, the joint inclination, and the internal friction angle.

Due to the high randomness of the distribution of the structural surface inclination in the gangue layer, a larger range of values is taken to cover as many structural surfaces as possible. After indoor tests, most of the values of the internal friction angle are around 30°, and the values are taken around this value. From the site work surface gangue thickness measurement can be seen, gangue thickness basically in 0.1 ~ 1.2 m between, so the value of the gangue thickness in the range to take the value. The density is taken mainly according to the density of the gangue relative to the coal body, which may be larger or smaller, so the value is taken around the density of the coal body. Combined with the actual situation and mining geological condition parameters of the Buertai coal mine, the horizontal values of the main influencing factors are determined, as shown in Table 2.

**Table 2** Horizontal values of main influencing factors

| Level | Factor | | | |
|---|---|---|---|---|
| | Density (g/cm$^3$) | Thickness (m) | Joint inclination (°) | Internal friction angle (°) |
| 1 | 1000 | 0.2 | 0 | 10 |
| 2 | 1350 | 0.4 | 20 | 20 |
| 3 | 1650 | 0.6 | 40 | 30 |
| 4 | 2000 | 0.8 | 60 | 40 |

In a sensitivity analysis of gangue parameters to the failure index of coal wall, the interaction between different factors is not considered. Therefore, the orthogonal table L16 ($4^5$) with 5 factors and 4 levels is used for scheme design, as shown in Table 3. The column numbers in the table are corresponding to the test factors, based on which the simulation test scheme of each main control factor is established.

## Results

### Sensitivity analysis of gangue parameter to rib spalling width

#### Variance analysis

The coal wall rib spalling is the damage phenomenon that occurs when the vulnerable area inside it is nurtured for a long time and develops to the limit of collapse. In order to reduce the influence of time and improve the reliability of the test results, the test results when the advancing distance is 50 m are selected here for analysis. According to the proposed numerical calculation model, the width of rib spalling under different test model, the width of rib spalling under different test conditions is obtained through simulation calculation. According to the orthogonal test theory, the simulation test data are analyzed and processed by variance analysis. The test results and data analysis are shown in Table 4.

In this table, $K_i$ is the sum of test indexes of the same level of each factor, $i = 1, 2, 3$; $T$ is the sum of $n$ test indexes; $C$ is a specific number of corrections,

**Table 3** Orthogonal design scheme

| Test number | Thickness (m) | Density (g/cm$^3$) | Inclination (°) | Internal friction angle (°) | |
|---|---|---|---|---|---|
| 1 | 1(0.2) | 2(1350) | 1(0) | 3(30) | 3 |
| 2 | 1 | 3(1650) | 4(60) | 2(20) | 4 |
| 3 | 1 | 4(2000) | 3(40) | 1(10) | 2 |
| 4 | 1 | 1(1000) | 2(20) | 4(40) | 1 |
| 5 | 2(0.4) | 4 | 1 | 1 | 2 |
| 6 | 2 | 1 | 2 | 4 | 3 |
| 7 | 2 | 2 | 3 | 3 | 1 |
| 8 | 2 | 3 | 4 | 2 | 4 |
| 9 | 3(0.6) | 1 | 2 | 4 | 1 |
| 10 | 3 | 2 | 3 | 1 | 2 |
| 11 | 3 | 3 | 4 | 2 | 4 |
| 12 | 3 | 4 | 1 | 3 | 3 |
| 13 | 4(0.8) | 2 | 3 | 1 | 2 |
| 14 | 4 | 3 | 4 | 2 | 4 |
| 15 | 4 | 4 | 1 | 3 | 3 |
| 16 | 4 | 1 | 2 | 4 | 1 |

**Table 4** Simulation test scheme and data analysis of rib spalling width

| Test scheme | Factor | | | | | Simulation results of rib spalling width (m) |
|---|---|---|---|---|---|---|
| | A | B | C | D | E | |
| | Thickness (m) | Density (g/cm$^3$) | Joint inclination (°) | Internal friction angle (°) | | |
| 1 | 1(0.2) | 2(1350) | 1(0) | 3(30) | 3 | 1.5 |
| 2 | 1 | 3(1650) | 4(60) | 2(20) | 4 | 2.1 |
| 3 | 1 | 4(2000) | 3(40) | 1(10) | 2 | 1.7 |
| 4 | 1 | 1(1000) | 2(20) | 4(40) | 1 | 1.7 |
| 5 | 2(0.4) | 4 | 1 | 1 | 2 | 1.6 |
| 6 | 2 | 1 | 2 | 4 | 3 | 1.5 |
| 7 | 2 | 2 | 3 | 3 | 1 | 2.5 |
| 8 | 2 | 3 | 4 | 2 | 4 | 1.7 |
| 9 | 3(0.6) | 1 | 2 | 4 | 1 | 2.3 |
| 10 | 3 | 2 | 3 | 1 | 2 | 2.5 |
| 11 | 3 | 3 | 4 | 2 | 4 | 2.4 |
| 12 | 3 | 4 | 1 | 3 | 3 | 1.7 |
| 13 | 4(0.8) | 2 | 3 | 1 | 2 | 2.5 |
| 14 | 4 | 3 | 4 | 2 | 4 | 2.6 |
| 15 | 4 | 4 | 1 | 3 | 1 | 2.0 |
| 16 | 4 | 1 | 2 | 4 | 3 | 2.6 |
| $K_1$ | 7.0 | 8.1 | 6.8 | 8.3 | 8.5 | $T=32.9$ |
| $K_2$ | 7.3 | 9 | 8.1 | 8.8 | 8.3 | |
| $K_3$ | 8.9 | 8.8 | 9.2 | 7.7 | 7.3 | |
| $K_4$ | 9.7 | 7 | 8.8 | 8.1 | 8.8 | |
| $K_{12}$ | 49.0 | 65.6 | 46.2 | 68.9 | 72.5 | $T^2=1082.4$ |
| $K_{22}$ | 53.3 | 81 | 65.6 | 77.4 | 68.9 | |
| $K_{32}$ | 79.2 | 77.4 | 84.6 | 59.3 | 53.9 | |
| $K_{42}$ | 94.1 | 49 | 77.4 | 65.6 | 77.4 | |
| $S_j$ | 1.2 | 4.7 | 0.6 | 0.1 | 0.3 | $C=67.7$ |
| $S_T$ | 7.6 | | | | | |
| $S_e$ | 0.8 | | | | | |

$C = T_2/n$; $S_j$ is the sum $\left(S_A S_B S_C\right)$ of squares of a factor, $S_j = \left(K_{12} + K_{22} + K_{32}\right)/3 - C$; $S_T$ is the sum of squares of total deviation, $S_T = \sum_{i=1}^{n} y_i^2$; and $S_e$ is the sum of squares of error deviation, $S_e = S_T - S_A - S_A - S_C$.

### Significance test

The ratio of the square sum of the average deviation of each factor to the square sum of the average deviation of the error is recorded as the $F$ value, which reflects the influence of each factor on the test results. The calculation formula of the $F$ value is:

$$F = \frac{S_j/f_j}{S_e/f_e} \tag{16}$$

where $S_j$ and $f_j$ are the sum of deviation squares and variance of each factor; $S_e$ and $f_e$ are the sum of squares of experimental error deviation and variance. According to Eq. (16), the $F$ values of factors A, B, C, and D can be calculated, respectively (Table 5).

In this table, (1) $F_{0.01}(4, 8) = 7.01$; $F_{0.05}(4, 8) = 3.84$; (2) when $S_j < 2S_e$, the calculated sum of deviation squares and variance are incorporated into the sum of deviation squares and variance, which are recorded as errors $e^{\Delta}$, so as to increase the sum of deviation squares and variance and improve the sensitivity of $F$ test; (3) $F > F_{0.01}(4, 8)$, this factor is highly significant, expressed in **; (4) $F_{0.05}(4, 8) < F < F_{0.01}(4, 8)$, this factor is significant, expressed by *; and (5) $F < F_{0.05}(4, 8)$, this factor is not significant. Table 7 shows the same results.

As shown in Table 5, the sensitivity analysis of various gangue parameters shows that factor A is highly significant, factor B and factor C are significant, and factor D is not significant. The influence of gangue parameters on the rib spalling width is A-C-B-D, that is, the sensitivity order of gangue parameters to the rib spalling width is gangue density > joint inclination > gangue thickness > internal

**Table 5** Variance analysis of rib spalling width

| Variance source | Sum of deviation square | Variance | Sum of average deviation squares | $F$ | $F_a$ | Significance |
|---|---|---|---|---|---|---|
| Thickness | 1.2 | 4 | 0.3 | 4 | $F_{0.05}(4, 8)$ | * |
| Density | 4.7 | 4 | 1.2 | 15.7 | $F_{0.01}(4, 8)$ | ** |
| Joint dip | 1.3 | 4 | 0.3 | 4.3 | $F_{0.05}(4, 8)$ | * |
| Internal friction angle | 0.1 | 4 | 0.03 | 0.3 | | |
| Error $e$ | 0.3 | 4 | 0.08 | | | |
| Error $e^{\Delta}$ | 0.4 | 8 | 0.05 | | | |

friction angle. It indicates that gangue density is the main influencing factor of rib spalling width of gangue-bearing coal seams. The increase of gangue density leads to the close arrangement of the structure of the gangue layer, the stability of the coal rock mass formed by the combination of gangue and coal body is improved, and the influence on the rib spalling width is reduced. Otherwise, the structural stability of the gangue layer decreases, the compressive strength of coal rock decreases, and the failure range of rib spalling increases.

## Sensitivity analysis of gangue parameters to rib spalling depth

### Variance analysis

When the advance distance is 50 m, the depth range of rib spalling is selected for data analysis. Table 6 shows the simulation test scheme, simulation test results, and data analysis of gangue parameters on the depth of rib spalling, and Table 7 shows the variance analysis for the significance test.

Through sensitivity analysis, it can be concluded that the influence of gangue density and joint inclination on the depth of coal walls is highly significant. The sensitivity of the internal friction angle to the rib spalling depth is significant, and the order of the gangue parameters is B-C-D-A, that is, the influence of the gangue parameters on the rib spalling depth is gangue density > joint inclination > internal friction angle > gangue thickness. It indicates that the main influencing factor of the rib spalling depth of gangue-bearing coal seams is gangue density. The increase of gangue density increases the compressive strength of the gangue layer itself and improves the stability of the coal rock mass formed by the gangue and coal body. When the gangue layer breaks, the extension distance is smaller. Otherwise, the structural stability of the gangue layer decreases, the compressive strength decreases, and the fracture extension distance of the gangue layer increases.

## Analysis of gangue density on stress distribution characteristics of coal body

According to the above sensitivity analysis, it is found that the gangue density has the greatest influence on the width and depth of the rib spalling. Limited to the space, the test numbered 5–8 is selected to analyze the influence of the gangue density on the stress distribution characteristics of the coal. When the advanced distance is 50 m in front of the coal wall, the stress distribution in the $x$-direction and $y$-direction is discussed.

As shown in Figs. 9 and 10, when the gangue density is 1000 g/cm$^3$ and 2000 g/cm$^3$, the stress difference in the $x$-direction is 4 MPa and 1 MPa at the gangue position, and the gangue density is small, there are more local stress concentration area, while the density is larger, the number and range of stress concentration areas are significantly decreased, indicating that with the increase of gangue density, its structural stability is improved, its resistance to failure is enhanced, and the stress distribution is relatively uniform. With the decrease of gangue density, the stress peak in the $y$-direction has a long lead distance. It indicates that as the density of gangue decreases, the hardness of gangue decreases gradually, and it is more prone to structural failure, resulting in the stress peak region in the $y$-direction moving forward. Therefore, under the same thickness of gangue, gangue density has a great impact on the stress distribution in the $x$- and $y$-directions in front of the coal wall. The greater the gangue density, the more uniform the stress distribution, the less damage caused by stress concentration, and the lower the risk of rib spalling.

## Discussion

In this study, the instability failure process and mechanical mechanism of gangue-bearing coal seams structure are analyzed, the sensitivity of different gangue parameters to rib spalling is discussed by numerical simulation, and the sensitivity of gangue parameters is evaluated by variance analysis and significance test.

**Table 6** Simulation test scheme and data analysis of rib spalling depth

| Test scheme | Factor | | | | | Test results (rib spalling depth/m) |
|---|---|---|---|---|---|---|
| | A | B | C | D | E | |
| | Thickness (m) | Density (g/cm$^3$) | Joint inclination (°) | Internal friction angle (°) | | |
| 1 | 1(0.2) | 2(1350) | 1(0) | 3(30) | 3 | 3.5 |
| 2 | 1 | 3(1650) | 4(60) | 2(20) | 4 | 3.2 |
| 3 | 1 | 4(2000) | 3(40) | 1(10) | 2 | 3.1 |
| 4 | 1 | 1(1000) | 2(20) | 4(40) | 1 | 2.3 |
| 5 | 2(0.4) | 4 | 1 | 1 | 2 | 1.2 |
| 6 | 2 | 1 | 2 | 4 | 3 | 3.1 |
| 7 | 2 | 2 | 3 | 3 | 1 | 3.2 |
| 8 | 2 | 3 | 4 | 2 | 4 | 2.2 |
| 9 | 3(0.6) | 1 | 2 | 4 | 1 | 2.1 |
| 10 | 3 | 2 | 3 | 1 | 2 | 3.3 |
| 11 | 3 | 3 | 4 | 2 | 4 | 4.3 |
| 12 | 3 | 4 | 1 | 3 | 3 | 1.2 |
| 13 | 4(0.8) | 2 | 3 | 1 | 2 | 2.9 |
| 14 | 4 | 3 | 4 | 2 | 4 | 3.3 |
| 15 | 4 | 4 | 1 | 3 | 1 | 1.2 |
| 16 | 4 | 1 | 2 | 4 | 3 | 3.5 |
| $K_1$ | 12.1 | 10.5 | 11.0 | 7.1 | 8.8 | $T=43.6$ |
| $K_2$ | 9.7 | 13.0 | 12.9 | 11.0 | 10.5 | |
| $K_3$ | 10.9 | 9.1 | 13.0 | 12.5 | 11.3 | |
| $K_4$ | 10.9 | 11.0 | 6.7 | 13.0 | 13 | |
| $K_{12}$ | 146.4 | 110.3 | 121.0 | 50.4 | 77.4 | $T^2=1901.0$ |
| $K_{22}$ | 94.1 | 169 | 166.4 | 121.0 | 110.3 | |
| $K_{32}$ | 118.8 | 82.8 | 169.0 | 156.3 | 127.7 | |
| $K_{42}$ | 118.8 | 121.0 | 44.9 | 169.0 | 169.0 | |
| $S_j$ | 0.73 | 6.5 | 5.4 | 2 | 2.3 | $C=118.8$ |
| $S_T$ | 16.9 | | | | | |
| $S_e$ | 2.3 | | | | | |

Significance test

**Table 7** Variance analysis of rib spalling depth

| Variance source | Sum of deviation square | Variance | Sum of average deviation squares | $F$ | $F_a$ | Significance |
|---|---|---|---|---|---|---|
| Thickness | 0.7 | 4 | 0.18 | 2.3 | | |
| Density | 6.5 | 4 | 1.6 | 21.7 | $F_{0.01}(4, 8)$ | ** |
| Joint dip | 5.4 | 4 | 1.4 | 18 | $F_{0.01}(4, 8)$ | ** |
| Internal friction angle | 2.0 | 4 | 0.5 | 6.7 | $F_{0.05}(4, 8)$ | * |
| Error $e$ | 2.3 | 4 | 0.6 | | | |
| Error $e^{\Delta}$ | 3.0 | 8 | 0.4 | | | |

In this study, the proposed mechanical model is mainly discussed under the homogenization of mechanical parameters such as gangue density and thickness. However, further research is needed under complex conditions such as non-uniformity of gangue distribution. For example, there are great differences in the thickness and density of the gangue layer with different spatial positions, while these parameters are simplified in our study. In addition, only the two-dimensional simulation of rib spalling is carried out, and the depth and width of rib spalling are discussed and analyzed in our study. The solution methods such

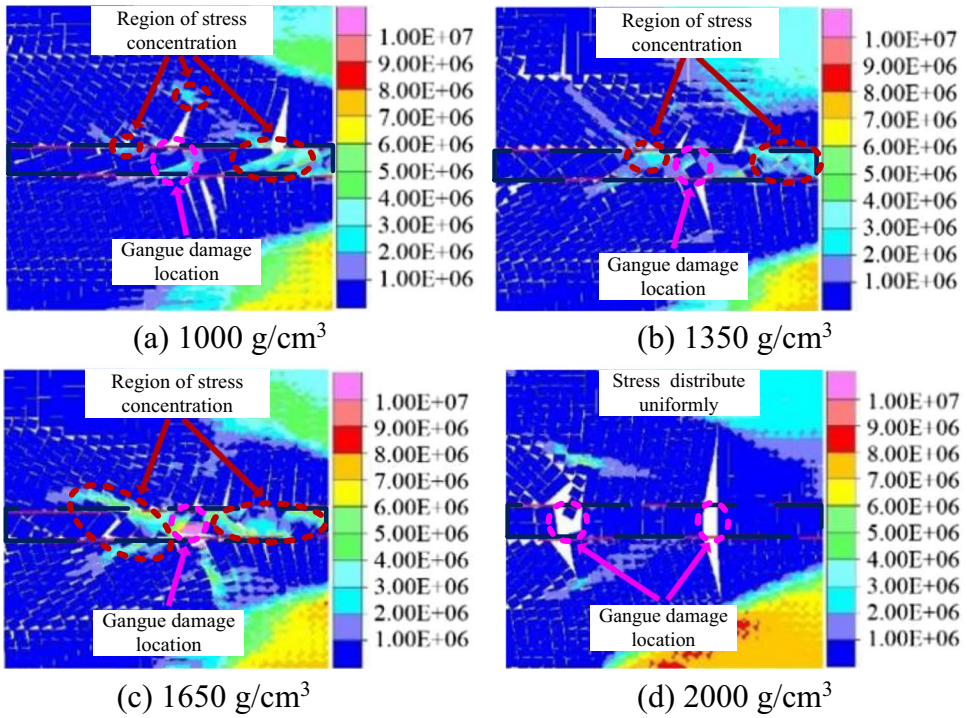


**Fig. 9** Stress nephogram in *x*-direction in front of coal wall

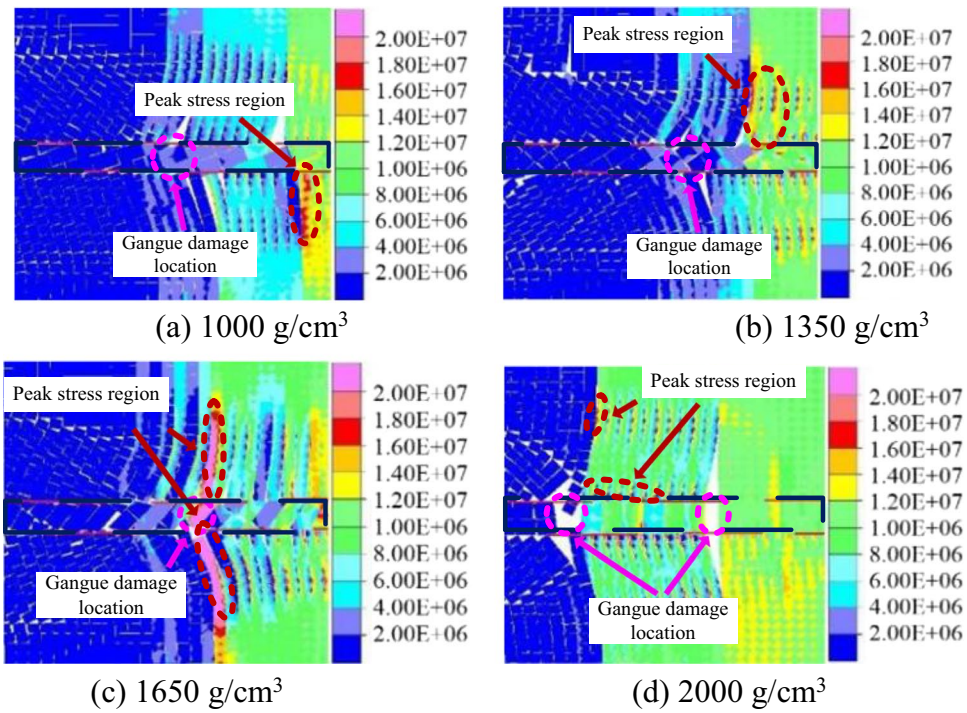


**Fig. 10** Stress nephogram in *y*-direction in front of coal wall

as spatial failure mode and influence range of rib spalling still need to be improved. In summary, new research methods are needed to further study and analyze the sensitivity of gangue parameters under complex conditions.

## Conclusion

In this study, the structural instability and failure process of gangue-bearing coal seams and the mechanical mechanism of gangue parameters on the rib spalling of gangue-bearing

coal seams are analyzed. The results show that the failure process of rib spalling is characterized by the fracturing failure of the lower coal body, shear failure of the gangue layer, and falling off of the upper coal body caused by gravity. Besides, the parameters such as thickness, density, joint inclination, and internal friction angle of gangue have a great influence on rib spalling.

Variance analysis and significance test are used to analyze the sensitivity of gangue parameters to the width and depth of rib spalling. It is concluded that the influence of gangue parameters on the rib spalling width is ordered as gangue density > joint inclination > gangue thickness > internal friction angle, and the influence of gangue parameter on the rib spalling depth is ordered as gangue density > joint inclination > internal friction angle > gangue thickness.

The gangue density has a great impact on the stress distribution in front of the coal wall. With the increase of the gangue density, the stress distribution tends to be more uniform, and the stress concentration hardly occurs, which reduces the risk of rib spalling.

**Author contribution** Guosheng Li: conceptualization, methodology, formal analysis, writing—original draft. Zhenhua Li: formal analysis, review and editing. Feng Du: formal analysis. Zhengzheng Cao: formal analysis.

**Funding** This work was supported by the National Natural Science Foundation of China (grant No.52174073, No.51774110, No.U1904128, No.52004082).

**Data availability** The datasets used or analyzed during the current study are available from the corresponding author on reasonable request.

## Declarations

**Ethics approval and consent to participate** Not applicable.

Consent for publication.
Not applicable.

**Competing interests** The authors declare no competing interests.

## References

Bai QS, Tu SH, Zhang XG, Zhang C, Yuan Y (2014) Numerical modeling on brittle failure of coal wall in longwall face-a case study. Arab J Geosci 7(12):5067–5080

Bai QS, Tu SH, Chen M, Zhang C (2016) Numerical modeling of coal wall spall in a longwall face. Int J Rock Mech Min 88:242–253

Behera B, Yadav A, Singh GSP, Sharma SK (2020) A numerical modeling approach for evaluation of spalling associated face instability in longwall workings under massive sandstone roof. Eng Fail Anal 117:104927

Chen K (2005) Experimental design and analysis. Tsinghua University Press, Beijing, pp 95–98

Diederichs MS, Kaiser PK, Eberhardt E (2004) Damage initiation and propagation in hard rock during tunnelling and the influence of near-face stress rotation. Int J Rock Mech Min Sci 41(5):785–812

Du K, Li XB, Li DY, Weng L (2015) Failure properties of rocks in true triaxial unloading compressive test. T Nonferr Metal Soc 25(2):571–581

Guo WB, Liu CY, Dong GW, Lv WY (2019) Analytical study to estimate rib spalling extent and support requirements in thick seam mining. Arab J Geosci 12(8):276

Kong DZ, Liu Y, Zheng SS (2019a) Sensitivity analysis of influencing factors and control technology for coalface failure. Arab J Geosci 12(17):550

Kong DZ, Cheng ZB, Zheng SS (2019b) Study on the failure mechanism and stability control measures in a large-cutting-height coal mining face with a deep-buried seam. B Eng Geol Environ 78(8):6143–6157

Lang D, Wu XB, Wu YP, Lin HF, Luo SH (2021) Boundary distribution of top-coal limit-equilibrium zone in fully mechanized caving in steeply dipping coal seams. Geomat Nat Haz Risk 12(1):2561–2589

Li GS, Li ZH, Du F, Cao ZZ (2020) Study on the failure characteristics of coal wall spalling in thick coal seam with gangue. Adv Civ Eng 2020:6668458

Li QC, Cheng YF, Ansari U, Han Y, Liu X, Yan CL (2022) Experimental investigation on hydrate dissociation in near-wellbore region caused by invasion of drilling fluid: ultrasonic measurement and analysis. Environ Sci Pollut R 29(24):36920–36937

Liu Y, Lu CP, Zhang H, Wang HY (2019) Numerical investigation of slip and fracture instability mechanism of coal-rock parting-coal structure (CRCS). J Struct Geol 118:265–278

Liu S, Yang K, Zhang T, Tang CN (2020) Rib spalling 3D model for soft coal seam faces with large mining height in protective seam mining: theoretical and numerical analyses. Geofluids 2020:8828844

Liu S, Yang K, Tang CA (2021) Mechanism and integrated control of "rib spalling: roof collapse-support instability" hazard chains in steeply dipping soft coal seams. Adv Mater Sci Eng 2021:5524591

Lu SF, Liu SF, Wan ZJ, Cheng JY, Yang ZZ, Shi P (2019) Dynamic damage mechanism of coal wall in deep longwall face. Adv Civ Eng 2019:3105017

Ma D, Duan HY, Zhang JX, Liu XW, Li ZH (2022a) Numerical simulation of water-silt inrush hazard of fault rock: a three-phase flow model. Rock Mech Rock Eng 55:5163–5182

Ma D, Duan HY, Zhang JX (2022b) Solid grain migration on hydraulic properties of fault rocks in underground mining tunnel: radial seepage experiments and verification of permeability prediction. Tunn Undergr Sp Tech 126:104525

Ma D, Duan HY, Zhang JX, Bai HB (2022c) A state-of-the-art review on rock seepage mechanism of water inrush disaster in coal mines. Int J Coal Sci Techn 9:50

Majdi A, Hassani FP, Nasiri MY (2012) Prediction of the height of destressed zone above the mined panel roof in longwall coal mining. Int J Coal Geol 98:62–72

Shabanimashcool M, Li CC (2012) Numerical modelling of longwall mining and stability analysis of the gates in a coal mine. Int J Rock Mech Min Sci 51:24–34

Shen MR, Chen JF (2006) Rock mechanics. Tongji University Press, Shanghai, pp 88–89

Song GF, Pan WD, Yang JH, Meng H (2015) Mining methods selection in thick coal seam based on fuzzy analytic hierarchy process. J Min Safety Eng 32(1):35–41

Tewari S, Kushwaha A, Bhattacharjee R, Porathur JL (2018) Crown pillar design in highly dipping coal seam. Int J Rock Mech 103:12–19

Wang ZH, Yang JH, Meng H (2015) Mechanism and controlling technology of rib spalling in mining face with large cutting height passing through fault. J China Coal Sci 40(1):42–49

Wang JQ, Zhang Q, Zhang JX, Liu HF, Zhu GL, Wang YB (2021) Study on the controller factors associated with roof falling and ribs spalling in deep mine with great mining height and compound roof. Eng Fail Anal 129:105723

Wu YP, Lang D, Xie PS (2016) Mechanism of disaster due to rib spalling at fully-mechanized top coal craving face in soft steeply dipping seam. J China Coal Sci 41(8):1878–1884

Xu YX, Wang GF, Li MZ, Xu YJ, Han HJ, Zhang JH (2021a) Investigation on coal face slabbed spalling features and reasonable control at the longwall face with super large cutting height and longwall top coal caving method. J China Coal Sci 46(02):357–369

Xu YX, Wang GF, Li MZ, Xu YJ, Zhou CT, Zhang JH (2021b) Mechanism of slabbed spalling failure of the coal face in fully mechanized caving face with super large cutting height. J Min Safety Eng 38(01):19–30

Yang PJ, Liu CY, Wu FF (2012) Breakage and falling of a high coal wall in a thick mined seam. J China Univer Min Tech 41(03):371–377

Yao QL, Li XH, Sun BY, Ju MH, Chen T, Zhou J, Liang S, Qu QD (2017) Numerical investigation of the effects of coal seam dip angle on coal wall stability. Int J Rock Mech Min 100:298–309

Yin SF, He FL, Cheng GY (2015) Study of criterions and safety evaluation of rib spalling in fully mechanized top-coal caving face with large mining height[J]. J China Univer Min Tech 44(05):800–807

Yu B, Zhao J, Kuang TJ, Meng XB (2015) In situ investigations into overburden failures of a super-thick coal seam for longwall top coal caving. Int J Rock Mech Min 78:155–162

Zhang WQ, Zhu XX, Xu SX, Wang ZY, Li W (2019) Experimental study on properties of a new type of grouting material for the reinforcement of fractured seam floor. J Mater Res Technol 8(6):5271–5282

Zhou H, Lu JJ, Xu RC, Zhang CQ, Meng FZ (2015) Critical problems of study of slabbing failure of surrounding rock in deep hard rock tunnel and research progress[J]. Rock Soil Mech 36(10):2737–2749

Zhu CQ, Fan H, Liu WR, Li SB (2021) Mechanical mechanism of water injection to enhance the stability of soft coal. Adv Mater Sci Eng 2021:9374217